ANALYSIS OF IMPROVED FUEL ROD MODELING IN COUPLED THERMAL-HYDRAULICS/NEUTRONICS CALCULATIONS

A. Jambrina, M. Yilmaz, M. Avramova and K. Ivanov
Department of Mechanical and Nuclear Engineering
The Pennsylvania State University
Reber Building, University Park, PA 16802, USA
azj128@psu.edu; mxo200@psu.edu; mna109@psu.edu; kni1@psu.edu

ABSTRACT

Best estimate codes are used to establish cycle operating limits to ensure that all NRC applicable requirements are met. Improved fuel thermal conductivity and the gap conductance models provide better prediction capability of fuel centerline temperatures, a licensing criterion in nuclear reactor safety and design analyses. Such models combine accuracy with efficiency, which will allow for the calculated margins or other limits to be less conservative than previously understood. The improved fuel temperature prediction results in improved evaluation of Doppler temperature used as a feedback parameter in coupled neutronics/thermal-hydraulic calculations.
.
The Modified Nuclear Fuel Industries (NFI) model for UO_2 fuel rods and Duriez/Modified NFI Model for MOX fuel rods have been implemented in the coupled thermal-hydraulic/neutronics codeCTF/NEM. This implementation accounts for the burnup and the Gadolinium content based on FRAPCON 3.4 instead of the MATPRO-11. In addition, the dynamic gap conductance model was pre-calculated with a fuel performance code and implemented in CTF/NEM using tables. This paper presents comparative analyses investigating the impact of the improved models on predictions of the feedback fuel (Doppler) temperature, and subsequently on power spatial distributions and total power time evolution.

The presented steady-state and transient analysis shows the effect of the thermal conductivity degradation (TCD) modeling on feedback effects in coupled thermal-hydraulic/neutronics calculations, specifically Doppler Temperature Coefficient (DTC) and eventually total core reactivity. The established OECD/NRC PWR MOX Rod Ejection Accident (REA) benchmark is utilized in the presented study.

KEYWORDS
Burnup and Gadolinium content, fuel-thermal-conductivity model, dynamic-gap- conductance model, feedback effects.

1. INTRODUCTION

In this paper, the study of the Rod Ejection Accident (REA), a design basis reactivity insertion accident for PWRs, is used to analyze the effect of improved fuel rod modeling in coupled thermal-hydraulics/neutronics code predictions. The improvements in fuel rod modeling are related to taking into account the fuel material (UOX vs. MOX), fuel burnup and presence of gadolinium burnable poisons in the fuel thermal conductivity and the gap conductance calculations. Improved fuel rod modeling results in improved prediction of fuel temperature and through feedback effects in improved prediction of power evolution and distributions.

A reactivity-insertion accident (RIA) is a nuclear reactor accident that involves an unwanted increase in fission rate and reactor power. The power increase may damage the reactor core, and in severe cases, even

lead to release of radioactivity in the environment. For these reasons nuclear regulatory organizations have established acceptance criteria for RIA, based on, initially, un-irradiated or moderately irradiated fuel, and nowadays, extended to higher fuel burnup.

The power excursion may lead to failure of the nuclear fuel rods and release of radioactive material into the primary reactor coolant. This material comprises gaseous fission products as well as fuel pellet solid fragments. In severe cases, the fuel rods may be shattered and large parts of the fuel pellet inventory dispersed into coolant. The expulsion of hot fuel into water has potential to cause rapid steam generation and pressure pulses, which could damage nearby fuel assemblies, other core components, and possibly also the reactor pressure vessel. These damage mechanisms are all related to high temperature, being the degree of fuel rod damage correlates well with the peak value of fuel pellet specific enthalpy. Regulatory acceptance criteria for RIA are traditionally formulated in terms of limits for the fuel radial average specific enthalpy, or the increment of this property during the RIA.

Recently a revision towards stricter acceptance criteria [1, 2] was made since several high burnup PWR fuel rods failed at remarkably low fuel enthalpies under RIA, in experimental test facilities. This revision was based on the effects of fuel burnup and residence time in the reactor. The fuel pellet material of primary concern is UO_2, but also is included $(U,Pu)O_2$ mixed oxide fuel, gadolinium-bearing burnable absorber fuel and inert matrix fuel. These experimental observations indicated the importance of taking into account the fuel material and burnup in modeling and simulation for realistic prediction of accident consequences. The objective of this paper is to investigate the effect of such model improvements.

2. ADDRESSED PHENOMENA

The main safety concerns in reactivity-insertion accidents are loss of long-term core cool-ability and possible damage to the reactor pressure boundary and the core through pressure wave generation [3, 4, 5]. From RIA simulation experiments in power pulse reactors, it has been found that the fuel rod behavior under a reactivity-insertion accident is affected primarily by the:

- Characteristics of the power pulse (amplitude and pulse width);
- Core coolant conditions (coolant pressure, temperature and flow rate);
- Burnup dependent state of the fuel rod. Among the most important properties are the pre-accident width of the pellet-clad-gap, the degree of cladding waterside corrosion, the internal gas overpressure in the fuel rod, and the distribution of gaseous fission products in the fuel pellets;
- Fuel rod design. Parameters of particular importance are the internal fill gas pressure, clad tube wall thickness, fuel pellet composition ($UO_2/PuO_2/Gd_2O_3$, enrichment) and the fuel pellet geometrical design (solid/annular).

These factors are important for the fuel rod behavior during an RIA, and they also control what kind of damage is inflicted to the fuel rod under the accident. Possible damage mechanisms are schematically presented in Fig.1.

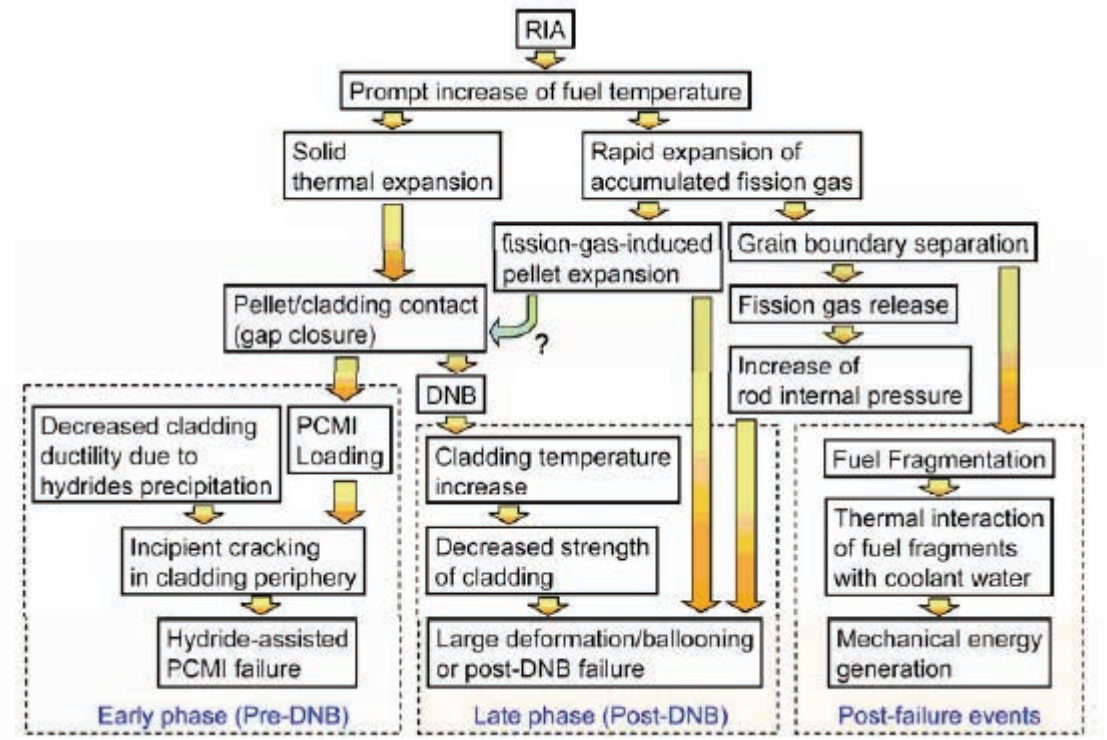

Figure 1. Possible mechanisms for fuel and cladding damage under an RIA [6]

There are four potential modes for the fuel rod behavior under an RIA:

- Low-temperature failures by Pellet-Cladding-Mechanical-Interaction (PCMI) under the early heat-up stage of the accident. This mode is relevant first and foremost to high burnup fuel rods with severely corroded cladding, which are subjected to a narrow power pulse, initiating from zero power conditions.

- High-temperature failures by cladding ballooning and burst. The failures occur as a consequence of film boiling and significant rod internal overpressure.

- Failures by disruption of the cladding upon quenching from high temperature. The failures occur as a as a consequence of oxygen-induced embrittlement due to high-temperature cladding oxidation under the film-boiling phase.

- High-temperature failures by melting of the cladding and possibly also of the fuel pellets.

For narrow power pulses, typical of PWR REAs, which initiate from zero power conditions, pulse reactor experiments show that the first of the above failure modes is usually the most restricting for high-burnup fuel rods, whereas either the second or the third failure is limiting for fresh and low-burnup fuel (the fuel design and coolant conditions decide whether clad ballooning or oxidation-induced embrittlement is most likely to cause the failure) [6]. All of these facts demonstrate that taking into account the fuel material and burnup not only in neutronics modeling (through cross-sections) but also in thermal-hydraulics calculations through the fuel rod model is very important for realistic estimation of accident consequences.

2.1. Fuel-Cladding Burnup Dependence

The microstructure and chemistry of fuel and cladding changes gradually over the life of a nuclear fuel rod because of irradiation damage, high temperature, mechanical stresses and chemical reactions. Following are mentioned the most important mechanisms occurring in the fuel-cladding during high burnup operations:

- Cladding degradation mechanisms:
    1. Uniform waterside corrosion which occurs on the outer surface of cladding. The zirconium in cladding chemically reacts with the water flowing around the cladding as coolant and developing a protective oxide on the surface of the cladding. In addition, crud deposition may happen.
    2. Hydriding which occurs when hydrogen generated by the corrosion reaction precipitates as zirconium hydride throughout the cladding thickness.
    3. Radiation damage that causes mechanical and geometrical properties of the material to change as a result of microstructural defects.
- Fuel pellet degradation mechanisms:
    1. Rim formation which is micro-structural evolution at high burnup on the fuel pellet periphery which increase the porosity.
    2. Micro-cracking in which the as-fabricated grain boundaries become brittle from the precipitation of fission gas bubbles and solid fission products at high burnup operations.
    3. Pellet-cladding interaction which occurs when a metallurgical and chemical bond starts forms between the cladding and the fuel during high burnup operations.

With increasing burnup, the above-described mechanisms cause changes to the macroscopic material properties, which are usually detrimental to the fuel behavior under RIAs. In order to perform an accurate fuel analysis, which reflects the above-described mechanisms, new capabilities are implemented in the CTF/NEM code [7] such as a thermal conductivity model that includes burnup and gadolinium content. The next paragraph explains the effects of thermal conductivity degradation.

2.2. Thermal Conductivity Degradation During High Burnup

Thermal conductivity of irradiated UO_2 is affected by the following changes that take place in the fuel during irradiation: solid fission product build up, porosity and fission gas bubble formation, and radiation damage [3, 4, 5]. The solid fission products formed during irradiation change the fuel lattice structure. The dissolved fission products lower the thermal conductivity while the precipitated fission products increase the thermal conductivity. The radiation damage generates additional defects in the lattice, especially in the cold regions of the fuel. The radiation damage from neutrons, alpha decay and fission increases the number of lattice defects and reduces the thermal conductivity of the fuel. In high burnup fuel operations, microstructural evolution is developed at the fuel pellet periphery (rim structure). It increases the porosity resulting in a decrease the fuel thermal conductivity on the pellet periphery and increase in the fuel temperature. Impurities and additives (gadolinium) decrease thermal conductivity like fission products, and in addition it has an impact on phonon-phonon scattering characteristic due to the mass difference.

In a summary, an important aspect of high burnup microstructure formation is the degradation of fuel thermal conductivity. The degradation is primarily caused by an increased resistance to phonon heat transport, as radiation damage and fission products accumulate in the crystal lattice. Theoretical models for thermal conductivity of solids, by which of porosity, grain size and lattice defects can be evaluated,

indicate that the thermal conductivity should decrease in the restructured fuel material as a consequence of grain subdivision and increased porosity. This degradation of fuel thermal conductivity with burnup is not being taken into account in the original fuel rod model of CTF/NEM. New thermal conductivity model has been implemented and tested in CTF/NEM and its effect on fuel temperature and power predictions during RIA is being studies in this paper.

3. CTF/NEM COUPLED CODE

The PSU/RDFMG version of COBRA-TF [8] (COolant Boiling in Rod Arrays-Two Fluid), CTF, is an advanced sub-channel code, which has the capability of three-field representation of two-phase flow model, which provides the thermal-hydraulic solution. The Nodal Expansion Method (NEM) code [9], is a few group, three dimensional (3-D) transient nodal core model, which provides the spatial kinetics solution.

3.1. Coupling Methodology

In order to provide solutions for accurate and efficient coupled calculations of operational transients and accidental scenarios, a coupling methodology [10] is required. Coupling methodologies are based on several basic criteria: coupling procedure, coupling implementation, appropriate spatial nodalization for the application, algorithms to exchange the time step in transient coupled calculations, numerical schemes of coupling between codes and schemes to control the convergence.

According to these criteria, the coupled code CTF/NEM [7] employs the following coupling methodology. Serial processing is employed with CTF as master code and internal integration scheme is utilized with NEM as a subroutine of CTF. The spatial nodalization schemes and mapping (overlays) are flexible and selected based on the computational cost and the accuracy of calculations. The temporal coupling between the codes is explicit. Fixed point iteration is utilized for steady state calculations. For transient calculations the time step size is determined by CTF an NEM can refine it based on its own time-step algorithm. CTF communicates with NEM by passing the spatial distributions of thermal hydraulic feedback variables such as fuel temperature (weighted using the temperature at the rod centers and surfaces in the radial and axial directions throughout the sub-channel node), moderator temperature and moderator density (averaged over all fluid phases present and weighted by void fraction), and boron concentration; and receiving the core power distribution, to be updated for the next CTF iteration/time-step. The coupled code can perform a steady-state solution, an automated k-search, and a transient simulation.

Fig 2. and Fig.3 show the steady-state and transient coupling schemes between CTF and NEM in coupled simulations.

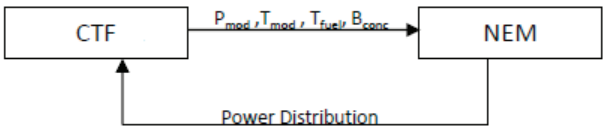

Figure 2. Steady-State Coupling Scheme [11]

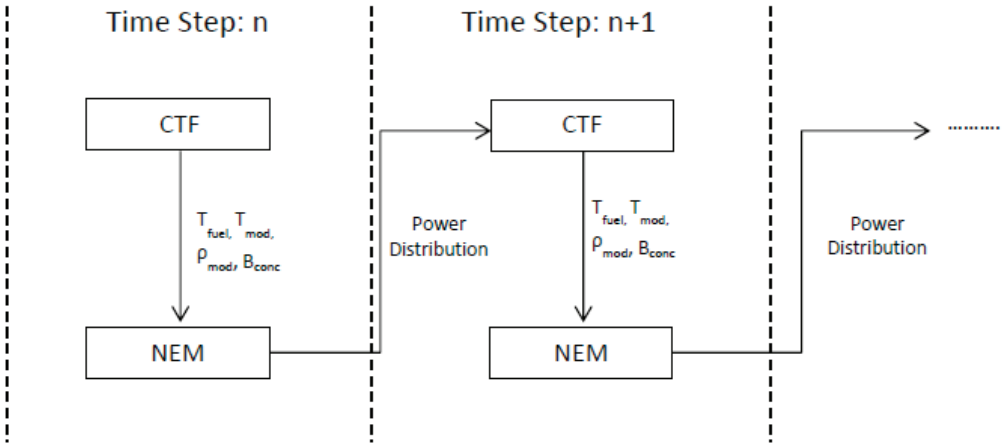

Figure 3. Transient Coupling Scheme [11]

Reactivity, ρ, is defined as the fractional departure from core criticality. Under reactor operation, the reactivity can be controlled, by movements of control rods or by addition/removal of soluble neutron absorbers in the coolant or moderator. However, reactivity is also affected by changes in fuel and moderator temperature, and by changes in the moderator void content,

$$\dot{\rho} = \dot{\rho}_{cs} + \frac{d\rho}{dT_f}\dot{T}_f + \frac{d\rho}{dT_m}\dot{T}_m + \frac{d\rho}{d\alpha_m}\dot{\alpha}_m \quad (1)$$

Where $\dot{\rho}_{cs}$ is the reactivity rate of change induced by reactivity control systems, $\dot{T}_f$ and $\dot{T}_m$ are the rates of temperature change for fuel and moderator, and $\dot{\alpha}_m$ is the rate of change for the moderator void volume fraction. Of the partial derivatives on the right hand side of the equation, the fuel temperature (Doppler) coefficient is always negative, which means that the fuel temperature increase accompanying a rise in reactivity always provides negative feedback, to the benefit of reactor stability. Moderator temperature and void coefficients can be either positive or negative depending on operating conditions. PWR generally operated with a negative moderator temperature coefficient, although the coefficient may turn positive in cases where the coolant is strongly borated and at low temperature; generally, reactivity can be inserted by a decrease in coolant temperature.

Continuing with the study of thermal conductivity degradation during high burnup, the changes on this parameter, as it has been explained above, affect directly the thermal-hydraulic solution and indirectly, the neutronics solution. The thermal conductivity model has an effect on prediction of the Doppler temperature, which is a fundamental feedback parameter in coupled thermal-hydraulic/neutronics calculations, is used in in the multi-dimensional linear surface interpolation to select the cross sections.

4. DEVELOPMENT OF BURNUP AND GADOLINIUM CONTENT DEPENDENT FUEL MODEL IN CTF/NEM

Since accurate predictions of fuel rod behavior is strongly dependent on temperature, the calculation of fuel thermal conductivity is critical [12, 13].

4.1. CTF Fuel Thermal Conductivity Model: MATPRO-11

CTF [8] uses MATPRO-11 correlation [14] to calculate the fuel thermal conductivity, which does not incorporate the impact of thermal conductivity degradation by burnup and gadolinium i.e. this model does not extend to high-burnup structure.

$$k_{UO_2} = \left[\max\left(0.0191, \frac{40.4}{(T-273.15)464.}\right) + 1.216 \times 10^{-4} * \exp\left(1.867 \times 10^{-3} * (T - 273.15)\right)\right] \quad (2)$$

where:

$k_{UO_2} = k_{95}$ = fuel thermal conductivity, W/m-°K
$T =$ temperature, K

Thermal conductivity is adjusted for as fabricated fuel density, d (100% TD), W/m-°K

$$k_d = k_{95} \times 100 \cdot \left[\frac{1-\beta(1-d)}{1-0.05\beta}\right] \quad (3)$$

where:

$\beta = 2.58 - (5.8 \times 10^{-4})(T - 273.15)$
$d =$ fuel theoretical density, in fraction of TD

4.2. FRAPCON 3.4 Fuel Thermal Conductivity Model: Modified NFI (UO2 fuels) and Duriez/Modified NFI (MOX fuels)

FRAPCON-3.4 [15] is a US-NRC fuel performance code which calculates the steady-state response of light-water reactor fuel rods during long term burnup conditions and also generates initial input conditions for transient fuel rod analysis code FRAPTRAN. The code computes the temperature, pressure, and deformation of a fuel rod as a function of time and includes the following models:

- heat conduction through fuel and cladding to the coolant;
- cladding elastic and plastic deformation;
- fuel-cladding mechanical interaction;
- fission gas release from the fuel and rod internal pressure;
- cladding oxidation.

The code also has material properties, water properties, and heat transfer correlations. FRAPCON-3.4 code uses single-channel coolant enthalpy rise model for the fuel rod thermal response calculations. The code also uses a finite difference approach in heat conduction model and FRAPTRAN which use a variable mesh spacing to accommodate the power peaking at the pellet edge which occurs in high burnup fuel operations.

FRAPCON-3.4 [15] has been validated for BWRs, PWRs, and heavy-water reactors [16]. The fuels that have been validated are uranium dioxide (UO_2), mixed oxide fuel (($U,Pu)O_2$), uranium-gadolinium (UO_2-Gd_2O_3), and UO_2 with zirconium diboride (ZrB_2) coatings. The cladding types that have been validated are Zircolay-2, Zircaloy-4, M5, and ZIRLO. FRAPCON-3.4 [15] can predict fuel and cladding temperature, rod internal pressure, fission gas release, cladding axial and hoop strain, and cladding corrosion and hydriding.

FRAPCON-3.4 uses Modified NFI [16] for UO_2 fuels and Duriez/Modified NFI [16] for MOX fuels based on Ohira and Itagaki formulation [17] and extends to high-burnup structures:

For UO_2 fuels:

$$k_{Mod\_NFI\_UO2} = \frac{1}{A + a*gad + BT + f(Bu) + \left(1 - 0.9\exp(-0.04Bu)\right)g(Bu)h(T)} + \frac{E}{T^2}\exp\left(-\frac{F}{T}\right) \quad (4)$$

where:

$k_{Mod\_NFI\_UO2} = k_{95}$ = thermal-conductivity for 95% dense fuel, W/m-K
$T =$ temperature, K
$Bu =$ burnup, GWd/MTU
$f(Bu) = 0.00187 * Bu$ = effect of fission products in crystal matrix (solution)
$g(Bu) = 0.038 * Bu^{0.28}$ = effect of irradiation defects.
$h(T) = \frac{1}{1+396\exp\left(-\frac{Q}{T}\right)}$ = temperature dependence of annealing on irradiation defects.
$Q = 6380$ K = temperature dependent parameter
$A = 0.0452$ m-K/W
$a = 1.1599$ constant
$gad =$ weight fraction of gadolinium
$B = 2.46 \times 10^{-4}$ m-K/W/K
$E = 3.5 \times 10^{9}$ W-K/m
$F = 16{,}361$ K

The thermal conductivity adjusted, k_d, for as fabricated fuel density d, based on Lucuta's correction [16], as fabricated 100% TD,), W/m-°K

$$k_d = 1.0789 \cdot k_{95} \cdot \left[\frac{d}{(1.0+0.5(1-d))}\right] \tag{5}$$

where:

$d =$ fuel theoretical density, in fraction of TD
$1.0789 =$ adjustment factor for conductivity at 100% TD

For MOX fuels:

$$k_{Duriez\_Mod\_NFI\_MOX} = \frac{1}{A(x)+a*gad+B(x)T+f(Bu)+\left(1-0.9\exp(-0.04Bu)\right)g(Bu)h(T)} + \frac{C_{mod}}{T^2}\exp\left(-\frac{D}{T}\right) \tag{6}$$

where:

$k_{Duriez\_Mod\_NFI\_MOX} = k_{95}$ = thermal-conductivity for 95% dense fuel, W/m-K
$T =$ temperature, K
$Bu =$ burnup, GWd/MTU
$f(Bu) = 0.00187 * Bu$ = effect of fission products in crystal matrix (solution)
$g(Bu) = 0.038 * Bu^{0.28}$ = effect of irradiation defects.
$h(T) = \frac{1}{1+396\exp\left(-\frac{Q}{T}\right)}$ = temperature dependence of annealing on irradiation defects.
$Q = 6380$ K = temperature dependent parameter
$a = 1.1599$ constant
$x = 2$ O/M
$A(x) = 2.85x + 0.035$ m-K/W
$B(x) = (2.86 - 7.15x) \times 10^{-4}$ m-K/W/K
$gad =$ weight fraction of gadolinium
$C_{mod} = 1.15 \times 10^{9}$ W-K/m
$D = 13520$ K

The thermal conductivity adjusted, k_d, for as fabricated fuel density d, based on Lucuta's correction [16], as fabricated 100% TD,), W/m-°K

$$k_d = 1.0789 \cdot k_{95} \cdot \left[\frac{d}{(1.0+0.5(1-d))}\right] \quad (7)$$

where:

d = fuel theoretical density, in fraction of TD
1.0789 = adjustment factor for conductivity at 100% TD

Incorporating the Modified NFI Model into CTF [8, 13] provides a new capability where the thermal conductivity degradation is calculated as function of burnup and gadolinium, achieving a better prediction of fuel temperature distribution within subchannel analysis.

5. COUPLED CODE BENCHMARKING AND VERIFICATION

The modifications introduced in fuel rod model have been qualified through code-to-code and code-to-data comparisons of standalone CTF in [13]. In this paper the effect of these modifications in coupled CTF/NEM analysis of the Purdue MOX/UO_2 Core Benchmark [18] is studied by evaluation of two steady states (HZP and HFP) and one transient - Exercise IV, rod ejection accident beginning from HZP conditions. This RIA event is of particular concern for MOX fueled cores since the delayed neutron fraction in MOX fuel is significantly smaller than in UO_2 cores. The rod ejection transient can result in significant, localized perturbations of the neutronics and thermal-hydraulic core parameters, which can be difficult for reactor core simulators to predict accurately, particularly in a heterogeneous MOX fueled core.

5.1. Purdue PWR MOX/UO_2 Core Model

Purdue MOX/UO_2 core benchmark [18] provides the framework to assess the capabilities of coupled codes to predict the transient response of a core partially loaded with MOX fuel. The core model is derived after a Westinghouse four-loop reactor core. It consists of 193 fuel assemblies which include 4.2 wt% and 4.5 wt% standard UO_2 assemblies as well as 4.0 wt% and 4.3 wt% MOX assemblies. The fuel assemblies consist of fresh, once-burned, and twice burned fuel assemblies with burn-up among the fuel assemblies ranging from 0.15 GWd/tHM to 37.5 GWd/tHM. The core is also enclosed by a single layer of neutron reflector assemblies in the radial and axial directions.

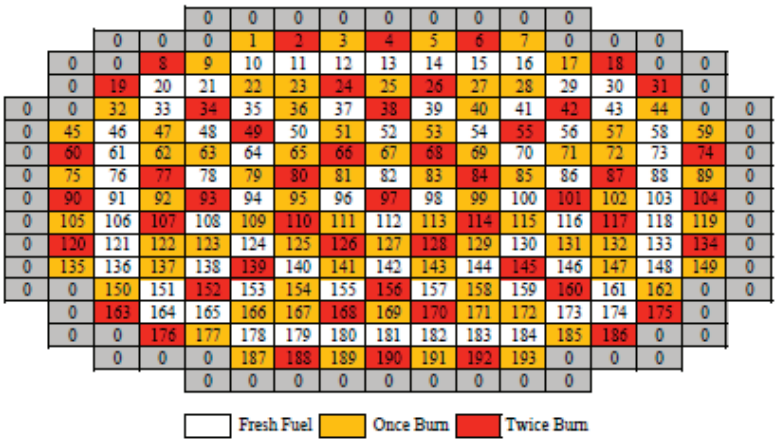

Figure 4. Radial Map used in NEM and CTF Models

The CTF model uses one sub-channel per fuel assembly for a total of 193 sub-channels. Although each fuel assembly contains 25 non-fuel rods in addition to the 264 fuel rods, only the fuel rods are modeled in CTF for each sub-channel by using the rod multiplier function. The non-fuel rods are neglected, but still accounted for in the sub-channel area and wetted perimeter. Finally, like the NEM model used, the CTF model divides the active fuel length into 26 axial nodes Fig. 4 gives the radial map used in the NEM and CTF discretization and spatial coupling overlays.

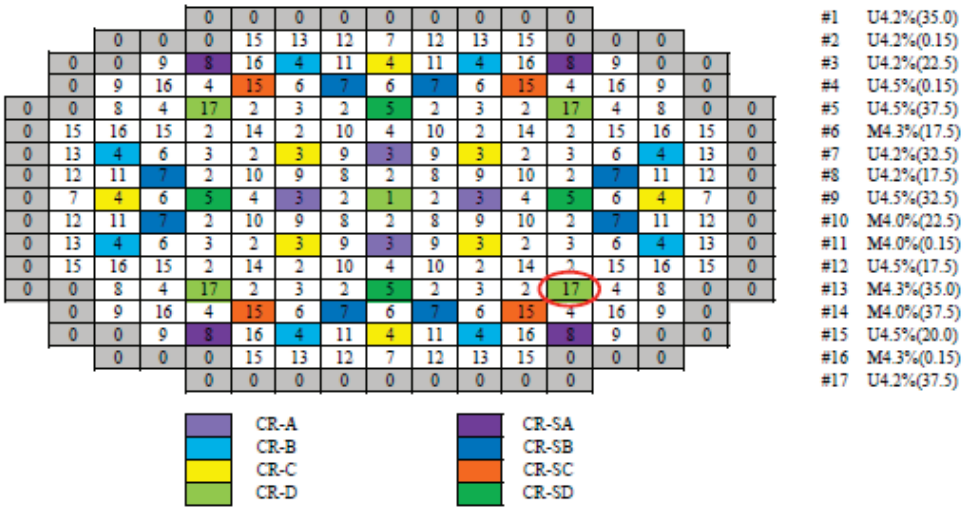

Figure 5. Material Compositions and Control Rod Bank Map

The nodalization scheme of the Purdue MOX/UO_2 core model used in NEM includes one node per fuel assembly in the radial directions for a total of 241 radial nodes. Axially, the core is divided into 28 layers, two of which are the top and bottom axial reflectors which are 21.42 cm thick. For the remaining 26 axial nodes, the active fuel length is divided into 26 equidistant axial nodes. The core is described by 17 fuel composition and an extra set for the reflector as shown in Fig. 5.

Selected core data and thermal-hydraulic values are listed in Table I.

Table I. Purdue MOX/UO_2 Core Design Parameters

Number of Fuel Assemblies	193
Core Full Power Rating [$MW_{thermal}$]	3565.0
Nominal Inlet Pressure [MPa]	15.5
Total Core Moderator Mass Flow Rate[kg/sec]	15849.4
HFP Core Average Moderator Temperature [K]	580.0
HFP Core Average Fuel Temperature[K]	900.0
HZP Core Average Fuel Temperature[K]	560.0
Fuel Lattice, Fuel Rods Per Assembly	17x17 Square,264
Control Rod Guide Tubes Per UO_2 Assembly	24
Guide Tubes Per Assembly	1
Active Fuel Length [cm]	365.76
Assembly Pitch [cm]	21.42
Pin Pitch [cm]	21.42
Core Load [tHM]	81.6
Shutdown Margin [%Dr]	1.3

The cross sections used are the same as those supplied by the benchmark specification, see Table I. They are two group multi-dimensional tabular cross section libraries, which are homogenized on the assembly level. A multi-dimensional linear surface interpolation is used to calculate the appropriate cross section based on the thermal hydraulic conditions supplied to NEM. The tabulated feedback parameters of the cross sections are moderator density, fuel temperature, and boron concentration. The only exception is the reflector nodes, which relies on boron concentration only for this particular cross section library.

Table II. Tabulated Cross Section Thermal-Hydraulic Range Purdue MOX/UO_2 Core

T-H Parameter	Minimum	Mid-Range	Maximum
Fuel Temperature [K]	560.0	900.0	1320.0
Moderator Density [g/cm^3]	0.66114	0.71187	0.75206
Boron Concentration [ppm]	0.0	1000.0	2000.0

5.1.1. Steady-state benchmark simulations: HFP (ARO) and HZP (ARI)

HFP (hot full power) conditions correspond to the core power of 100.0 % rated power (3565 MW), inlet coolant temperature of 560 K, inlet pressure of 15.5 MPa, with all rods out (ARO).

HZP conditions correspond to the core power of 10^{-4} % rated power, inlet coolant temperature of 560 K, inlet pressure of 15.5 MPa, with all rods in (ARI, all control banks in and all shutdown banks out)

Without actual operating and measured data available, the benchmark reference solutions for Part II (steady-state HFP conditions) and Part III (steady-state HZP conditions) were based on the results of the Purdue Advanced Reactor Core Simulator (PARCS) code using two energy (2G) groups.

5.1.2. Transient benchmark simulation: rod ejection accident (HZP conditions)

The highest worth rod is assumed to be fully ejected in 0.1 seconds after which no reactor scram is considered. The control rod ejection is to be performed from HZP (all control banks in, all shutdown banks out), and critical boron concentration. During the entire calculation the boron concentration and the position of the other control rods are assumed to be constant. The transient is to be calculated for 1.0 sec.

5.2. Coupled Code Verification

The strategy employed to verify the new capability of CTF/NEM coupled code starts with benchmarking against the Purdue MOX/UO_2 Core benchmark at steady-state and transient conditions. The reference in this study will be PARCS 2G neutronics code. PARCS uses its own simplified one-dimensional PWR thermal-hydraulic feedback model and for this benchmark utilizes the provided in benchmark specifications simplified thermal conductivity properties for UO_2 and MOX fuels:

$$k_{UO2} = 1.05 + \frac{2150}{T-73.15}\ [\frac{W}{m\cdot K}] \quad (5)$$

$$k_{MOX} = 0.9k_{UO2} \quad (6)$$

In order to quantify the effect of the addition of the new thermal conductivity fuel rod model (Modified NFI), the results of the CTF/NEM are also compared to the MATPRO-11 fuel rod model (CTF model).

5.2.1. Steady-state calculation: HFP (ARO) and HZP (ARI)

Table III. HFP Steady-State Summary

	Critical Boron Concent. [ppm]	Assembly Power Error		Core Average T/H Properties		
		%PWE	%EWE	Doppler Temperature [K]	Moderator Density [kg/m^3]	Moderator Temperature [K]
PARCS 2G (Ref.)	1679.30	-	-	836.00	706.10	581.10
CTF/NEM (MATPRO-11)	1669.01	0.60414	0.82493	848.78	703.08	580.76
CTF/NEM (Modified NFI)	1649.24	0.60233	0.94843	873.24	703.99	580.39

As shown in Table III for the HFP case, both versions of the CTF/NEM, with MATPRO-11 and Modified NFI model, agree with the critical boron concentration of the benchmark solution with a difference of 0.62% and 1.79 % respectively. For both cases, the power-weighted error and error-weighted error are similar and less than 1%. The moderator density and temperature have values with a positive low difference with respect the reference (0.42% and 0.29%, for moderator density, MATPRO-11 and Modified NFI model respectively; and 0.05% and 0.12%, for moderator temperature, MATPRO-11 and Modified NFI model respectively). The Modified NFI model introduces a higher difference in the Doppler temperature respect the reference (37.24 K, or 4.26% more) than the MATPRO-11 model (12.78 K, or 1.23%). Fig. 6a represents the axial power distribution for the three cases, and Fig. 6b gives the quarter core radial power distribution results.

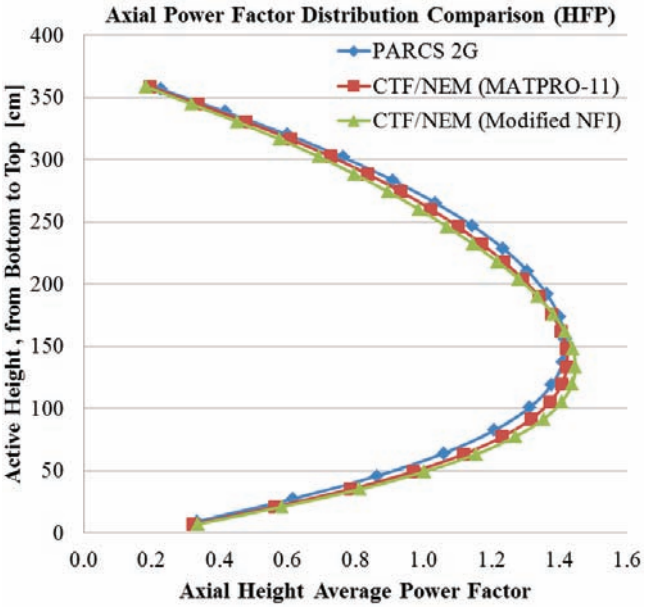

1.0923	1.3702	1.1873	1.3674	1.0139	1.1172	1.1176	0.4861
1.0975	1.3846	1.1917	1.3768	1.0101	1.1021	1.1147	0.4832
1.0826	1.3687	1.1791	1.3701	1.0076	1.1068	1.1266	0.4876
1.3702	1.2521	1.0696	1.1966	1.3011	0.9730	1.1149	0.5795
1.3847	1.2606	1.0724	1.1876	1.3064	0.9715	1.0968	0.5784
1.3684	1.2449	1.0606	1.1815	1.3062	0.9749	1.1087	0.5841
1.1873	1.0696	1.1685	1.3344	1.209	1.1925	1.1124	0.4846
1.1922	1.0727	1.1695	1.3449	1.2099	1.1793	1.1147	0.4806
1.1779	1.0598	1.1592	1.3404	1.2097	1.1855	1.1268	0.4851
1.3674	1.1966	1.3344	1.0656	1.2893	1.1796	1.0056	0.4015
1.3779	1.1885	1.3455	1.0575	1.2970	1.1849	0.9962	0.3990
1.3673	1.1794	1.3389	1.0541	1.2995	1.1917	1.0067	0.4028
1.0139	1.3011	1.2090	1.2893	0.9316	1.1229	0.6446	
1.0113	1.3078	1.2109	1.2976	0.9322	1.1317	0.6500	
1.0045	1.3025	1.2069	1.2977	0.9336	1.1398	0.6550	
1.1172	0.9729	1.1924	1.1796	1.1229	0.8409	0.3185	
1.1039	0.9729	1.1808	1.1860	1.1322	0.8339	0.3181	
1.1020	0.9708	1.1813	1.1885	1.1382	0.8402	0.3201	
1.1176	1.1149	1.1123	1.0056	0.6446	0.3185		
1.1169	1.0988	1.1165	0.9975	0.6505	0.3182		
1.1207	1.1031	1.1218	1.0030	0.6535	0.3198		
0.4861	0.5795	0.4846	0.4015		PARCS 2G		
0.4841	0.5794	0.4814	0.3996		CTF/NEM (MATPRO-11)		
0.4851	0.5812	0.4830	0.4013		CTF/NEM (Modified NFI)		

Figure 6. a) Radially Averaged Core HFP Axial Power Distributions; b) Axially Averaged Core HFP Radial Power Distributions (1/4 Core)

The analysis of the HZP case shows smaller differences between the two versions of CTF/NEM caused by a lower power level and thus a lower importance of the fuel rod model and any modifications in it. A lower difference is found between the reference and CTF/NEM about critical boron concentration, 0.33%, as it is shown in Table IV.

Table IV. HZP Steady-State Summary

	Critical Boron Concent. [ppm]	Assembly Power Error		Core Average T/H Properties		
		%PWE	%EWE	Doppler Temperature [K]	Moderator Density [kg/m^3]	Moderator Temperature [K]
PARCS 2G(Ref.)	1340.71	-	-	560.00	752.00	560.00
CTF/NEM (MATPRO-11)	1345.16	0.61140	0.95183	559.16	752.81	559.16
CTF/NEM (Modified NFI)	1345.16	0.61140	0.95183	559.16	752.81	559.16

The results given in Fig. 7a and Fig. 7b for the axial and radial power distribution confirm that the effect of the new thermal conductivity fuel rod model implemented in CTF/NEM is not as pronounced at HZP conditions as at HFP conditions (see Fig. 6a and Fig. 6b)

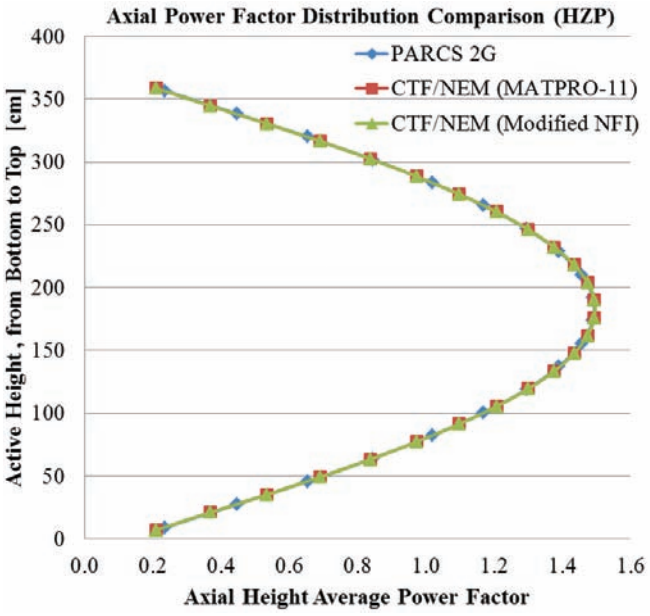

0.3484	0.7861	0.5152	1.5072	1.3119	1.1721	0.4989	0.2945
0.3455	0.7889	0.5114	1.5069	1.3050	1.1582	0.4958	0.2941
0.3455	0.7889	0.5114	1.5069	1.3050	1.1582	0.4958	0.2941
0.7861	0.8083	0.7992	1.3621	1.7479	1.0829	0.8327	0.3894
0.7889	0.8034	0.8008	1.3466	1.7454	1.0822	0.8247	0.3864
0.7889	0.8034	0.8008	1.3466	1.7454	1.0822	0.8247	0.3864
0.5153	0.7992	0.6141	1.5691	1.6421	1.3580	0.5661	0.3315
0.5114	0.8008	0.6077	1.5761	1.6465	1.3455	0.5651	0.3325
0.5114	0.8008	0.6077	1.5761	1.6465	1.3455	0.5651	0.3325
1.5072	1.3621	1.5692	1.3164	1.6260	1.4633	1.0494	0.3694
1.5069	1.3466	1.5761	1.3073	1.6371	1.4747	1.0489	0.3675
1.5069	1.3466	1.5761	1.3073	1.6371	1.4747	1.0489	0.3675
1.3119	1.7480	1.6421	1.6260	0.6272	1.3738	0.8220	
1.3050	1.7454	1.6465	1.6371	0.6246	1.3952	0.8363	
1.3050	1.7454	1.6465	1.6371	0.6246	1.3952	0.8363	
1.1721	1.0829	1.3581	1.4633	1.3738	1.0867	0.4274	
1.1582	1.0822	1.3455	1.4747	1.3952	1.0822	0.4275	
1.1582	1.0822	1.3455	1.4747	1.3952	1.0822	0.4275	
0.4989	0.8327	0.5661	1.0494	0.8220	0.4274		
0.4958	0.8247	0.5651	1.0489	0.8363	0.4275		
0.4958	0.8247	0.5651	1.0489	0.8363	0.4275		
0.2945	0.3894	0.3315	0.3694				
0.2941	0.3864	0.3325	0.3675				
0.2941	0.3864	0.3325	0.3675				

PARCS 2G
CTF/NEM (MATPRO-11)
CTF/NEM (Modified NFI)

Figure 7. a) Radially Averaged Core HZP Axial Power Distributions; b) Axially Averaged Core HZP Radial Power Distributions (1/4 Core)

5.2.2. Transient calculation: rod ejection accident (HZP conditions)

Table V. Comparison of Peak Time, Peak Power and Peak Thermal Properties

	Peak Time [sec]	Peak Power [%]	Peak Reactivity [$]	Peak Doppler Temperature [K]	Peak Moderator Density [kg/m^3]	Peak Moderator Temperature [K]
PARCS 2G(Ref.)	0.335	142.00	1.120	566.80	752.21	560.06
CTF/NEM (MATPRO-11)	0.335	192.95	1.127	567.80	752.77	559.18
CTF/NEM (Modified NFI)	0.340	193.93	1.128	567.76	752.76	559.18

A comparison of peak time, peak power, peak reactivity and peak thermal-hydraulic properties (Doppler temperature, moderator density and moderator temperature) is shown in Table V.

The difference between the peak power predicted by PARCS and CTF/NEM (both versions) respectively, is explained with the differences in the coupling methods and feedback models. CTF/NEM is a coupled code and PARCS is a neutronics code with internal simplified 1-D PWR thermal-hydraulic model. The rod ejection occurs from 0.0 sec to 0.1 sec and results in a large and narrow pulse. Small differences in the models result in changes of peak reactivity.

The following figures show the time evolution of the core power (Fig. 8) and feedback parameters (Doppler temperature, Fig. 9; moderator density, Fig. 10; and moderator temperature, Fig. 11).

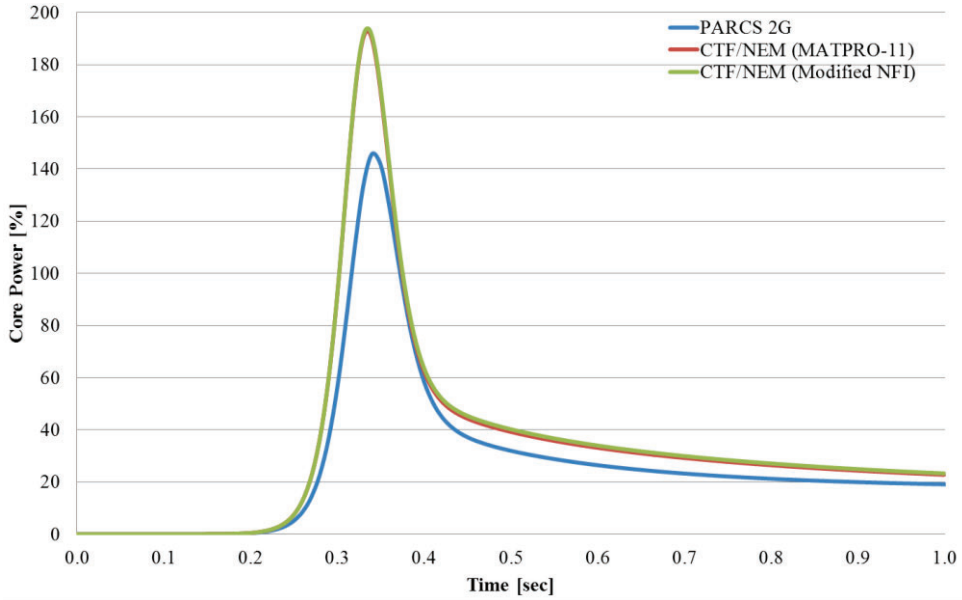

Figure 8. Core Power (%) Time Evolution

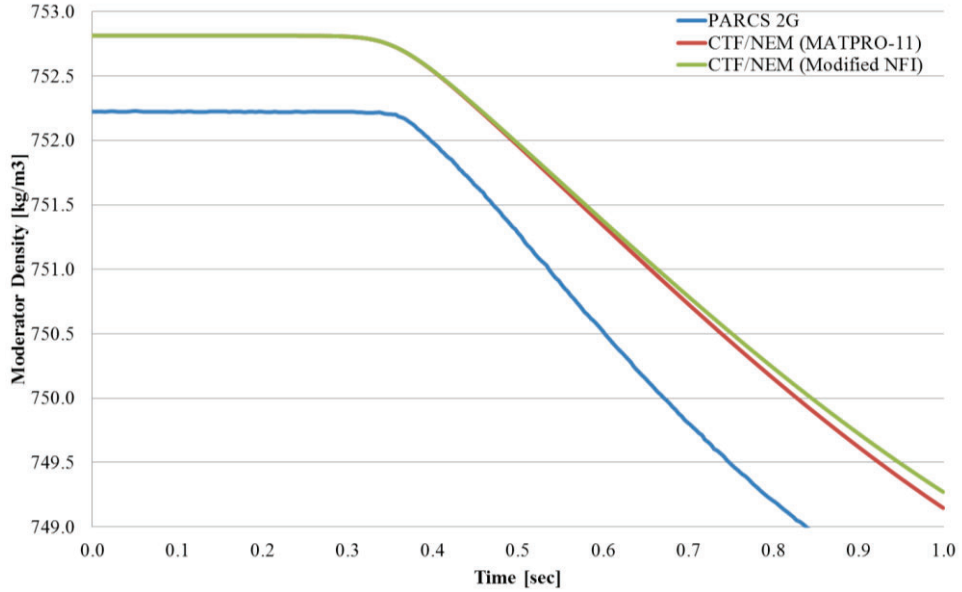

Figure 9. Moderator Density Time Evolution

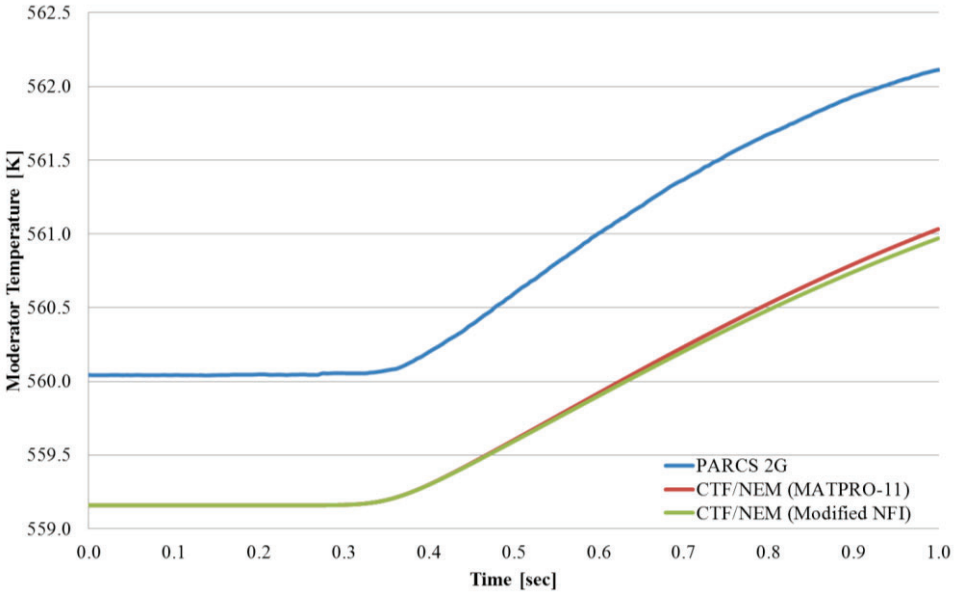

Figure 10. Moderator Temperature Time Evolution

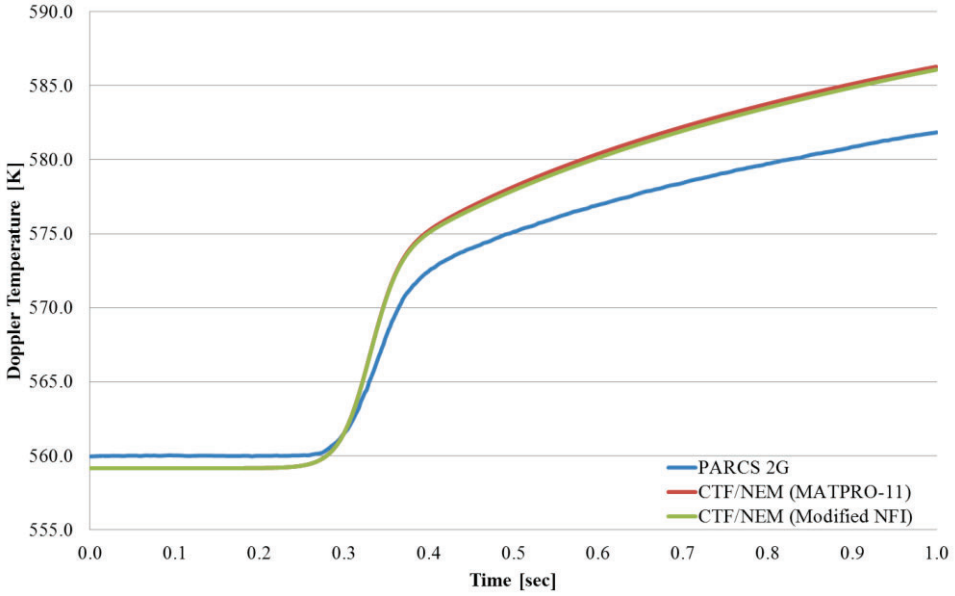

Figure 11. Doppler Temperature Time Evolution

The feedback parameter that is directly affected by the modification of the thermal conductivity correlation in the fuel rod model is the Doppler temperature. The change in prediction of this parameter causes changes in power. For that reason Doppler temperature and the core power have been analyzed for both models (MATPRO-11 and Modified NFI model) at the peak time. Moderator properties are similar in the three cases. Fig. 12 shows the axial power factor distribution and axial Doppler temperature distribution at peak time.

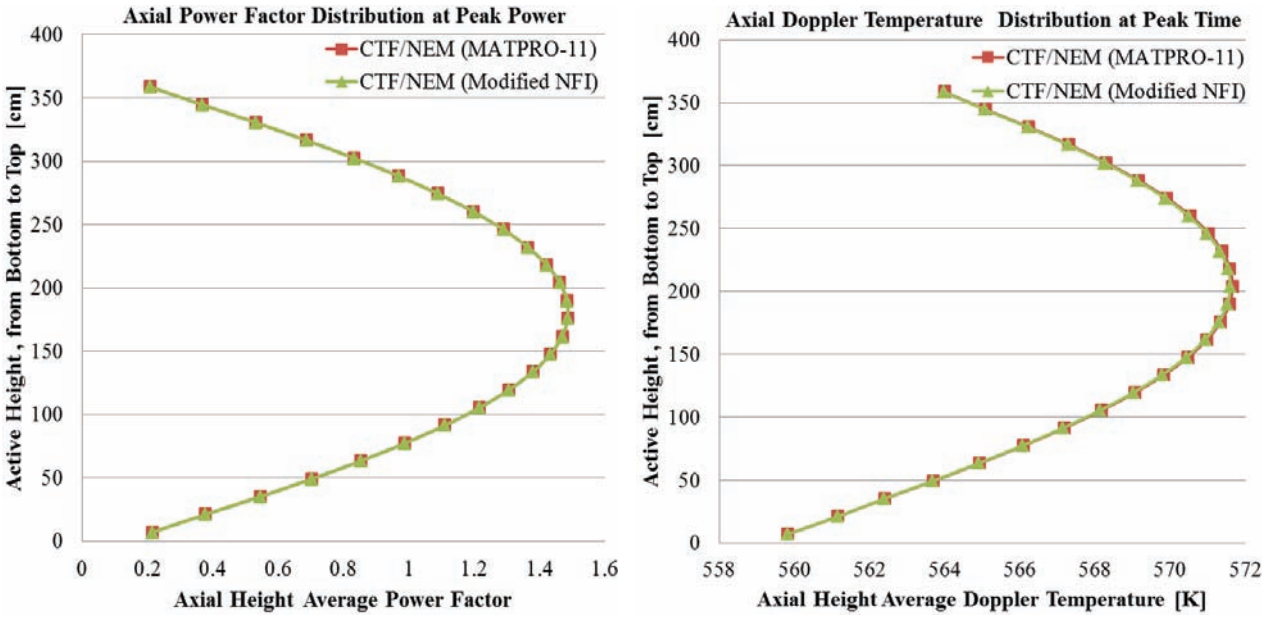

Figure 12. a) Radially Averaged Core Axial Power Distributions at Peak Time; b) Radially Averaged Doppler Temperature Axial Power Distributions at Peak Time

Fig. 13 and Fig. 14 show, respectively, the axially average differences of core radial power distributions and the axially averaged differences of Doppler temperature distributions at peak time, between MATPRO-11 and Modified NFI models, using MATPRO-11 as reference.

				0.01%	0.00%	0.00%	0.00%	0.00%	0.00%	0.00%				
			0.01%	0.01%	0.01%	0.01%	0.01%	0.01%	0.01%	0.01%	0.01%	0.00%		
		0.01%	0.01%	0.02%	0.01%	0.01%	0.01%	0.02%	0.01%	0.02%	0.02%	0.01%	0.01%	0.01%
		0.01%	0.02%	0.00%	0.02%	0.02%	0.02%	0.01%	0.02%	0.02%	0.02%	0.01%	0.01%	0.00%
	0.01%	0.01%	0.01%	0.02%	0.02%	0.01%	0.01%	0.01%	0.01%	0.01%	0.01%	0.01%	0.00%	0.00%
	0.00%	0.01%	0.01%	0.02%	0.01%	0.01%	0.00%	0.00%	0.01%	0.00%	0.01%	0.01%	0.00%	0.00%
	0.00%	0.01%	0.01%	0.02%	0.01%	0.00%	0.01%	0.01%	0.00%	0.00%	0.00%	0.00%	0.00%	0.00%
	0.00%	0.01%	0.02%	0.01%	0.01%	0.00%	0.01%	0.00%	0.00%	-0.01%	-0.01%	-0.01%	-0.01%	-0.01%
	0.00%	0.01%	0.01%	0.02%	0.01%	0.01%	0.00%	0.00%	0.00%	-0.01%	-0.02%	-0.03%	-0.02%	-0.01%
	0.00%	0.01%	0.02%	0.02%	0.01%	0.00%	0.00%	-0.01%	-0.01%	-0.01%	-0.03%	-0.04%	-0.03%	-0.01%
	0.00%	0.01%	0.02%	0.02%	0.01%	0.01%	0.00%	-0.01%	-0.02%	-0.03%	-0.04%	-0.05%	-0.04%	-0.02%
		0.01%	0.01%	0.01%	0.01%	0.01%	0.00%	-0.01%	-0.03%	-0.04%	-0.05%	-0.04%	-0.03%	-0.02%
			0.01%	0.01%	0.00%	0.00%	0.00%	-0.01%	-0.02%	-0.03%	-0.04%	-0.03%	-0.03%	-0.01%
			0.01%	0.00%	0.00%	0.00%	0.00%	-0.01%	-0.01%	-0.01%	-0.02%	-0.02%	-0.01%	
					0.00%	0.00%	0.00%	-0.01%	0.00%	0.00%	-0.01%			

Figure 13. Axially Averaged Differences of Relative Core Radial Power Distribution [in %] at Peak Time between MATPRO-11 and Modified NFI models (MAPRO-11 as reference)

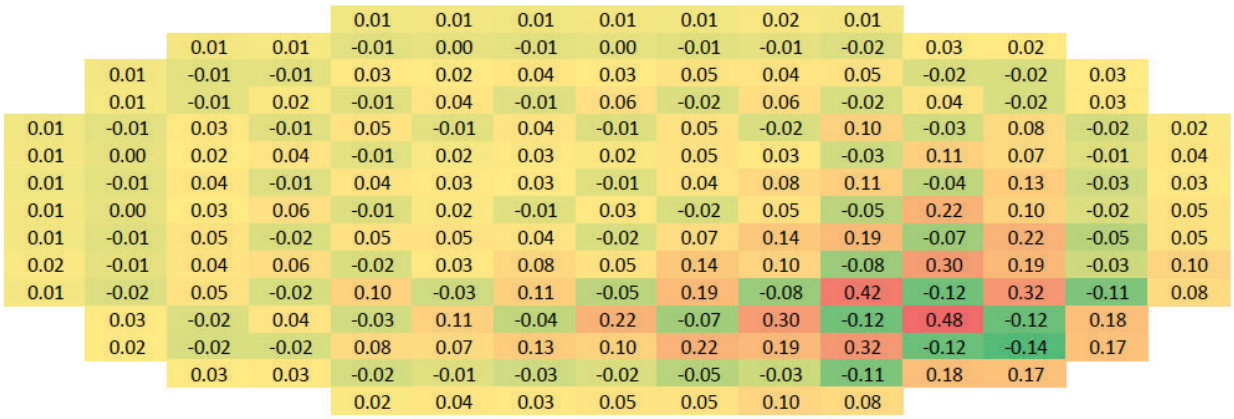

Figure 14. Axially Averaged Difference of Doppler Temperature Radial Power Distribution [in K] at Peak Time between MATPRO-11 and Modified NFI models (MAPRO-11 as reference)

The maximum difference in the radially averaged relative core power at peak time is -0.05% and the maximum difference in the radially average Doppler temperature at peak time is 0.48 K. The fact that small differences are being observed between the two different fuel rod models during the rod ejection transient could be explained with the HZP initial state. The power level is very low (almost negligible) and changes in fuel rod modeling do not play an important role.

6. CONCLUSIONS

The new capability implemented in the CTF/NEM coupled code, which is based on the Modified NFI model for thermal conductivity calculation, allows to obtain accurate results taking into account the real fuel behavior corresponding to its burnup and feed material composition. The analysis presented in this paper investigates the effect of considering thermal conductivity degradation with burnup on predictions of HZP and HFP steady states and Rod Ejection transient starting from a HZP state. The effect of taking into account the thermal conductivity degradation of high-burnup fuel is more pronounced at HFP steady state and less important for HZP steady state and Rod Ejection transient starting from HZP state. As a future work analysis of a Rod Ejection transient starting from a HFP state is planned combined with a sensitivity studies on the other important sub-model of the fuel rod model – gap-gas conductance model.

The obtained results indicate that the effect of thermal conductivity degradation with increasing fuel burnup reduces the safety margin of a nuclear power plant. It is necessary to improve the safety analysis methods using coupled codes with improved fuel conductivity models. Applying the improved coupled code CTF/NEM to the Purdue MOX/UO_2 core benchmark helps to quantify the effect of the newly implemented improved models on the results of safety analysis and contributes to further enhancing of best-estimate coupled tools leading to predictions of more realistic safety margins.

REFERENCES

1. USNRC, Standard Review Plan §4.2, Fuel System Design, Appendix B, Interim Acceptance Criteria and Guidance for the Reactivity Initiated Accidents, NUREG-0800 (March 2007).
2. C. Vitanza and M. Hrehor, *Review of High Burn-up RIA and LOCA Database and Criteria*, Report NEA/CSNI/R(2006)5, OECD Nuclear Energy Agency, Committee on Safety of Nuclear Installations, Paris, France (2006).
3. E.B. Boyack *et al*., *Phenomenon Identification and Ranking Tables (PIRTs) for Rod Ejection Accidents in Pressurized Water Reactors Containing High Burnup Fuel*, NUREG/CR-6742, for the U.S. Regulatory Commission, Washington D.C., USA (2001).
4. F.T. Fuketa and F. Nagase and T. Sugiyama, "RIA- and LOCA-Simulating Experiments on High Burnup LWR Fuels", *IAEA Technical Meeting on Fuel Behavior Modelling under Normal, Transient and Accident Conditions and High Burnups*, Kendal, United Kingdom, September 5-8 (2005).
5. M. Ishikawa and S. Shiozawa, "A Study of Fuel Behavior under Reactivity-Inserted Accident Conditions", *Journal of Nuclear Materials*, **95**, pp. 1-30 (1980).
6. C.J. Luxat and D.R. Novog, "A Generalized Failure Map for Fuel Elements Subject to a Power Pulse", *19th International Conference on Structural Mechanics in Reactor Technology (SMiRT-19),* Toronto, Canada, August 12-19, (2007).
7. RDFMG/MNE/PSU, "CTF/NEM Coupled Code", Technical Report, RDFMG, The Pennsylvania State University, USA (2015).
8. RDFMG/MNE/PSU, "CTF - A Thermal Hydraulic Subchannel Code for LWRs Transient Analysis. User's Manual", Technical Report, RDFMG, The Pennsylvania State University, USA (2015).
9. RDFMG/MNE/PSU, "NEM User's Manual", Technical Report, RDFMG, The Pennsylvania State University, USA (2012).
10. A. Jambrina *et al*. "Peach Bottom Turbine Trip Benchmark Analysis with TRAC-BF1/PARCS and TRACE/PARCS Coupled Codes", *The 15th International Topical Meeting on Nuclear Reactor Thermal - Hydraulics,(NURETH-15),* Pisa, Italy, May 12-17 (2013)
11. M. Biery, *Investigation of Coupled Code Pressurized Water Reactor Simulations using CTF with Soluble Boron Tracking*, MSc Thesis, The Pennsylvania State University, USA (2013).
12. S.H. Ryu, K.S. Um and J.I. Lee, "Effect of Thermal Conductivity Degradation for High-Burnup Fuel during a Postulated Control Element Assembly Ejection Accident", *KEPCO Nuclear Fuel*, **242**, pp. 305-353 (2014).
13. M. Yilmaz, *Development of Burnup Dependent Fuel Rod Model in COBRA-TF*, PhD Thesis, The Pennsylvania State University, USA (2014).
14. L.D. Hagman and A.G. Reymann, *MATPRO-Version 11 A Handbook of Materials Properties for Use in the Analysis of Light Water Reactor Fuel Rod Behavior*, NUREG/CR-0497 (TREE-1280), prepared by EG&G Idaho, INC., Idaho Falls, ID, for the U.S. Nuclear Regulatory Commission, Washington D.C., USA (1979).
15. J.K. Geelhood, G.W. Lusher and E.C. Beyer, *FRAPCON-3.4: A Computer Code for the Calculation of Steady-Stae Thermal-Mechanical Behavior of Oxide Fuel Rods for High Burnup*, NUREG/CR-7022 vol. 1, PNNL-19418, Pacific Northwest National Laboratory, Richland, Washington, USA (2011).
16. G.W. Lusher and J.K. Geelhood, *Material Property Correlations: Comparisons between FRAPCON-3.4, FRAPTRAN 1.4 and MATPRO*, NUREG/CR-7024, PNNL-19417, Pacific Northwest National Laboratory, Richland, Washington, USA (2010).
17. K. Ohira and N. Itagaki, "Thermal Conductivity Measurements of High Burnup UO_2 Pellet and a Benchmark Calculation of Fuel Center Temperature", *Proceedings of the ANS International Topic Meeting on LWR Fuel Performance*, Portland, Oregon, March 2-6, 1997, pp. 541-549 (1997).
18. T. Kozlowski and T. Downar, *PWR MOX/UO_2 Core Transient Benchmark: Final Report,* NEA/NSC/DOC(2006)20, (2006).